



Convection and Climate: What Have We Learned from Simple Models and Simplified Settings?

Dennis L. Hartmann¹ · Peter N. Blossey¹ · Brittany D. Dygert¹

Published online: 6 June 2019
© Springer Nature Switzerland AG 2019

Abstract

Purpose of Review We ask what fundamental insights about the relationship of tropical convection to climate have arisen from recent investigations using simplified models.

Recent Findings The vertical distribution of relative humidity should remain approximately constant in a changed climate. The temperature of clouds in the upper troposphere should also remain effectively constant for climate changes likely to occur in response to human-induced warming. The fractional coverage of convective clouds will likely decrease slightly with warming, but it is not known how the albedo and net radiative effect of tropical convective clouds will change. The areal extent and net radiative effect of tropical convective clouds depend on the interactions of radiation, cloud physics, and turbulence within the extended upper-level ice clouds. SST gradients develop naturally as a result of the aggregation of convection and large-scale thermodynamics and circulation act to couple the cloud properties and the SST.

Summary Radiative-convective equilibrium continues to provide insight into the structure and energy balance of the atmosphere by incorporating the interactions among radiation, cloud physics, and atmospheric motion.

Keywords Climate sensitivity · Tropical convection · Radiative-convective equilibrium · Cloud feedback · Cloud modeling

Introduction

Since the pioneering work of Manabe and Wetherald [1], it has been known that much of importance about the response of the atmosphere to climate change can be learned by studying radiative-convective equilibrium (RCE). Radiation heats the surface and cools the atmosphere, convection results, and the role of moisture in the equilibration process is paramount. Manabe and Wetherald [1] made an assumption of fixed relative humidity, based on observations of the seasonal cycle in middle latitudes, and this assumption has proved to be fairly robust by subsequent data analysis [2] and model experimentation [3]. The dependence of the primary infrared absorber on temperature makes the outgoing longwave radiation (OLR) fairly linear in temperature, compared to saturation vapor

pressure [4]. Simple theory based on the entraining plume model helps to explain the observed tropical humidity distribution but still requires that the precipitation efficiency be specified and entrainment and detrainment profiles approximated with idealized high-resolution simulations [5]. In realistic three-dimensional situations, however, the relative humidity of the free troposphere does vary spatially, and this structure may play an important role in climate sensitivity [6]. The large-scale structure of humidity in the tropics seems to be reproducible from simple trajectory modeling [7–9].

Possible changes in the relative area of moist and dry regions that might occur as climate changes have been a topic of considerable interest. Simple energetic arguments suggest that the upward mass flux in convection should decline in a warmed Earth [10]. The vertical gradient of moisture increases exponentially with warming, so that vertical motion releases more latent energy per unit of mass flux, but the capacity of the atmosphere to cool by radiative emission is a weak linear function of surface temperature [11, 12]. The tendency of convection to aggregate in a limited portion of the available area has been shown using models with both explicit and parameterized convection in a radiative-convective equilibrium setting [13]. Also, convection becomes deeper in a

This article is part of the Topical Collection on *Convection and Climate*

✉ Dennis L. Hartmann
dhartm@uw.edu

¹ Department of Atmospheric Sciences, University of Washington, Seattle, Washington, USA

warmed Earth, in consequence of the basic physics of radiative-convective equilibrium in which water vapor is the primary longwave emitter [14–16]. While we can make some substantial arguments for why warming may cause the area of deep convection to decrease, the intensity of deep convection to increase, and the temperature at cloud top to remain the same, at present, we have very little robust theory for explaining how the net radiative effects and net feedback effects of tropical convective clouds may change in a warmed Earth. This requires a comprehensive theory for how the optical properties of convective cloud systems will change in a warmed Earth, and in particular, the abundance and optical properties of extended anvil clouds that are usually associated with tropical convection. This will likely require treating the interaction of radiation, turbulence, and microphysics within the extended anvil clouds [17–19], which has not been a strong focus of climate modeling efforts. In coupled atmospheric-ocean simulations in which SST gradients and large-scale circulations interact with convection, it is apparent that the deep convective clouds and the boundary layer clouds are linked both through the vertical and horizontal structure of the coupled system.

Convection in a Box

An important form of process model experimentation has been the simulation of radiative-convective equilibrium above fixed sea surface temperature (SST) in a limited area, but with high spatial resolution and interactive radiation and cloud physics. RCE is calculated in a limited domain, but the cloud-scale motions are resolved. Such simulations are the twenty-first century equivalent of the state-of-the-art in the 1960s, in which the motions were represented by a fixed maximum lapse rate and conservation of energy. Early examples of the modern approach to RCE are Held et al. [20] and Tompkins and Craig [21]. The lapse rate, the relative humidity, and the cloud properties are explicitly calculated, rather than being specified at the outset. Problems remain, of course, in that the answer depends on the spatial resolution, domain size, and the parameterizations of radiation, sub-grid-scale turbulence, and cloud microphysics. Nonetheless, RCE-in-a-box simulations provide the opportunity to ask more basic questions and to test theories and parameterizations.

It appears that RCE is most directly applicable to the Tropics, and most high-resolution simulations have been set in the tropical context. The relaxation time is controlled by radiative transfer, which constrains the subsidence velocities [22]. The adjustment to imposed SST variations tends toward a moist adiabatic lapse rate, the relative humidity is insensitive to SST, and the humidity and cloud distributions tend to just shift upward with warmer SST [15, 23]. Under otherwise homogeneous forcing, convection in a sufficiently large box organizes itself within the box into stable convective and non-

convective regions, a process often called self-aggregation [24, 25]. The processes through which convection aggregates in an otherwise uniform domain and the potential importance of this for climate have become topics of great currency.

Water Vapor Feedback

Water vapor feedback is the most important positive feedback in the climate system, but is somewhat sensitive to an assumption of constant relative humidity. This assumption has been tested by simulating the observed response to a volcanic eruption with a global climate model [3], but the question of why the relative humidity is fixed is still often asked. The vertical structure of relative humidity can be simulated with an RCE-in-a-box model of arbitrary complexity to show that the vertical structure of relative humidity is approximately fixed as a function of temperature. A simple model for why the relative humidity remains fairly constant can then be constructed that will reproduce the prediction of a model that includes the interactions between motions and cloud physics in a realistic manner [5]. The theory requires the specification of the fractional entrainment and detrainment rates but predicts that the relative humidity will be an invariant function of temperature as the climate warms.

Self-Aggregation of Convection

Convection typically collects in a part of the domain that becomes moist and cloudy, while other regions of the domain have little or no convection and the atmosphere is drier. This organization of convection within the domain of a model evolves naturally, even with uniform SST and starting from a homogeneous initial perturbation, and occurs for both parameterized and explicit convection and in both two- and three-dimensional simulations [20, 26, 27]. Random organization is enhanced because moist regions are more favorable for continued convection than regions that are dry. The most robust reason for this self-aggregation feedback appears to be the radiative effects of upper-tropospheric water vapor and clouds [13, 28], although surface turbulent fluxes and circulations connecting the convecting and non-convecting regions also play a critical role, and some simulations show a strong role of the radiative effect of low clouds [29]. Other work suggests an important role for a “moisture memory” mechanism [30, 31] and cold pool formation [32].

Experiments with simple models suggest that states with aggregated convection have lower climate sensitivity than states that are not aggregated. One reason for this is because the average relative humidity of the free troposphere is decreased by aggregation, so that water vapor feedback is weaker in an aggregated state. Experiments with limited-area cloud-resolving models suggest that aggregation is more likely at higher SST [28], but once aggregated, the degree of

aggregation is not that sensitive to temperature change [33]. It is therefore unclear whether further aggregation in a warmer world will be a major contributor to climate sensitivity, since tropical convection may already be fully aggregated.

Intensity of Convection

The rain rate is greater in the Tropics than midlatitudes, and it is hypothesized that the rain rate will increase in a warmed Earth. Global mean precipitation is constrained by the radiative cooling rate of the atmosphere to increase at less than the Clausius-Clapeyron (CC) rate ($1\text{--}3\%K^{-1}$ compared to $\sim 7\%K^{-1}$ for CC) [11], but the distribution of precipitation in space and time is very important and will likely change as the climate warms. Practically important characteristics of the precipitation distribution include not only the mean amount and the intensity, but also the statistics of the duration of high precipitation events [34].

Convection-resolving simulations tend to support the idea that warmer temperatures lead to greater intensity of rainfall, but it is unclear whether the highest rates increase at the CC rate, less or more. One idea for understanding this is to use a cloud-resolving model, which can better represent the small-scale motions and their interactions with microphysics and radiation. Some such work suggests that the scaling for extreme precipitation is not materially different from the CC rate [35, 36]. Microphysical processes such as hydrometeor fall speed also affect precipitation intensity [37]. The thermodynamic contribution is much more uniform than the dynamic contribution, which is scale and location dependent [38]. Nie et al. [39] suggest that the availability of more latent heat in a warmer climate will drive stronger motions in convectively driven systems and cause the precipitation intensity in some systems to increase more than the CC thermodynamic rate would suggest [40].

Insight into possible linkages between radiative-convective equilibrium and precipitation intensity may be provided by the entraining plume model [40–43]. Singh and O’Gorman [41] used a simple entraining plume model in the limit of zero buoyancy [44] to show that as the temperature increases, the Convective Available Potential Energy (CAPE) increases, even for a fixed entrainment rate. The physical reason is that the effect of entrainment of dry air increases with temperature because the difference in specific humidity between the saturated plume and its environment increases with temperature. Therefore, the equilibrium lapse rate exceeds the moist adiabatic lapse rate increasingly as the climate warms, and CAPE increases. The model agrees reasonably well with cloud-resolving model simulations and observations.

Singh and O’Gorman [41] leave us with the countervailing conclusions that as the climate warms, entrainment becomes a bigger drag on convective plumes, but that the temperature differences between rising undilute parcels and their

environment will be increased in a warmer world. It may be that the convection can organize itself to take advantage of the greater CAPE, or that the availability of more CAPE will simply allow those parcels or plumes that by chance do not entrain as much to gain greater velocity on their way up. Either way, the extreme precipitation rates could increase. Cloud-resolving model simulations suggest that greater updraft velocities are achieved at upper levels in a warmer climate, but not at the rate predicted by the increase in CAPE [40], so some balance between enhanced CAPE and enhanced entrainment cooling of upward-moving parcels determines the answer. That balance could depend on modeling details like resolution and synoptic-scale organization of mesoscale convection.

Atmospheric Cloud Radiative Effect

A current direction in climate research is to investigate how atmospheric radiative heating changes associated with the presence of clouds impact both clouds and their environment. Both experiments with cloud-resolving models in a limited domain and experiments with global climate models have been conducted. It is well known that boundary-layer stratocumulus is strongly dependent on radiative cooling at cloud top [45]. Intercomparison projects with global climate models have also been designed to look into the global importance of the Atmospheric Cloud Radiative Effect (ACRE) [46]. The radiative heating associated with high clouds can have a substantive influence on the position of the ITCZ [47] and on the poleward shift of the storm tracks in global warming simulations [48]. These provide an interesting complement to studies in which the SST is allowed to respond to the cloud effects. The shortwave and longwave cloud effects on circulation and SST changes can then be diagnosed with cloud-locking experiments, in which the clouds from a warming simulation are applied to the control simulation and vice versa [49, 50]. Such experiments show the potential of cloud radiative effects on the atmosphere and surface to alter the positions of the jet streams and their associated circulation features.

Tropical convective anvil clouds have large effects on the longwave and shortwave energy fluxes at the top of the atmosphere. Recent work with cloud-resolving models of convective anvils indicates that their properties are highly affected by the strong radiative heating associated with them. Elevated ice clouds in the Tropics are strongly heated by longwave radiation absorption at cloud base and may also be cooled by radiation near their tops. This drives instability in the cloud layer that may interact strongly with turbulence and cloud microphysics within the ice layer [18, 51]. It appears that the balance between the positive cloud radiative effect of thin anvil ice clouds and negative effect of thick, rainy anvil clouds is critical to the small effect these clouds have on the current radiation balance of Earth [19]. This distribution of thin and thick anvil cloud resulting from tropical convection does not seem

to be well simulated by climate models [52], and much more work is needed to understand the relative abundance of thick and thin ice clouds in the Tropics and how that ratio might change with climate.

Fixed Temperature at the Top of the Well-Mixed Troposphere

Chemical and other evidence suggests that the well-mixed layer of the tropical troposphere ends well below the tropopause defined by the minimum temperature. Ozone begins to increase toward stratospheric values around 14 km [53]. This implies that the detrainment of ozone-depleted air from the lower troposphere begins to decrease well before the cold-point tropopause is reached. It is hypothesized that this occurs because radiative cooling by longwave emission from water vapor becomes ineffective at temperatures colder than about 220 K, since the saturation vapor density is so low at those temperatures and the cooling there comes primarily from the strongest rotational lines of water vapor [14]. If radiation cannot cool the atmosphere efficiently, then any upward energy transport by convection will stabilize the atmosphere, it will take longer for radiation to destabilize the atmosphere, and convection will reach those altitudes less frequently. The argument rests on the radiative relaxation time increasing in the upper tropical troposphere because of the low specific humidity [54], and that convective heating must be balanced by radiative cooling. Because the lapse rate approaches dry adiabatic in the upper tropical troposphere, small changes in lapse rate are associated with large changes in stability and should be expected near the top of the well-mixed layer. Such lapse rate changes have been described by Folkins [55]. The lapse rate changes are a reflection of the transition from a well-mixed to a partially mixed troposphere that occurs around 220 K in the Tropics.

These facts led to the “fixed anvil temperature” (FAT) hypothesis, that the temperature of tropical anvil clouds that occur near the top of the well-mixed troposphere should remain roughly constant as the climate changes. This is because the saturation vapor density is purely a function of temperature, and the rotational lines of water vapor that emit in the upper troposphere are not that sensitive to pressure broadening. As the FAT hypothesis was intended to inform the discussion of high cloud responses to global warming over tropical oceans, it assumes weak convection and near-equilibrium conditions as are found in the present climate. Weak convection suggests that the convection is relatively free of the influence of convection driven by surface features and that the neutralizing effect of evaporation in updrafts is active. An approximate balance between convective, radiative, and large-scale heating is implied by the near-equilibrium conditions. Thus, the FAT hypothesis would not be expected to “hold” over land where convection can be disequilibrated,

nor in a very cold climate where the convection becomes essentially dry and the surface mixed layer extends to the top of the troposphere. The original FAT hypothesis also assumes that the atmospheric cloud radiative effects are small or apply only in a limited area, or act in such a way to reinforce the clear-sky radiative constraint. However, recent work suggests that ACRE may have a significant role in the lifetime of anvil cirrus [18], so that ACRE may not be a negligible factor in FAT.

Hartmann and Larson [14] used a mesoscale model with parameterized convection to show that for tropical conditions, the cloud top temperature varies much less than the temperature at a fixed pressure in the upper troposphere and less than the surface temperature. The surface temperature was varied over a range of 6 K, which is more than the warming expected from human-induced climate change. The temperature change at a fixed pressure of 200 hPa was about 13 K, because the model approximately followed the moist adiabatic lapse rate. This temperature change at 200 hPa was compared with three other discrete temperatures: the temperature where the optical depth of cloud reached 0.1 in the convective region, the temperature where the radiative cooling rate had decreased to 0.5 K day^{-1} from its mid tropospheric value of about 1 K day^{-1} , and the temperature where the large-scale pressure velocity in the convective region peaked. All three of these temperatures varied by not more than about 2 K, an order of magnitude less than the temperature at a fixed pressure.

All else being equal, a near-constant cloud top temperature would produce a positive feedback, since the emission temperature of the clouds becomes decoupled from the surface temperature. This hypothesis has been supported by RCE-in-a-box simulations [15] and by global climate models [16]. Harrop and Hartmann [56] used a cloud-resolving model in RCE to show that the clouds could be moved vertically to different temperatures by changing the water vapor amount only in the radiation scheme, indicating that the temperature dependencies of the cloud microphysics in the model are not the fundamental constraint on cloud top temperature. They also showed that the radiative effects of carbon dioxide and especially ozone can cause the clouds to warm a little with surface warming, but that if water vapor is the only radiatively active gas, then the cloud temperature remains very nearly constant as the surface temperature is increased.

Recently, this concept has been extended to the globe, suggesting that the temperature of the extratropical tropopause is also constrained to a nearly fixed temperature related to the saturation specific humidity [57]. A mechanistic study using simplified global climate models suggests that this hypothesis has validity and confirms the radiative role of water vapor in constraining the temperature of the extratropical tropopause [58].

Several papers have argued that other mechanisms are responsible for the presence of extended ice clouds in the upper tropical troposphere and have questioned the importance of

water vapor cooling in constraining the depth of convection. Seeley et al. [59] argue that ice cloud fraction peaks in the upper troposphere because evaporation is an inefficient sink of condensed water there due to the low saturation-specific humidity at those low temperatures. In the lower troposphere, mixing with environmental air causes rapid evaporation due to the larger saturation deficit of the warmer lower tropospheric air. Therefore, if condensed water is supplied at the same rate at all levels, the cloud fraction will still be top heavy, since in the upper troposphere evaporative decay becomes slow and the removal of cloud is constrained by the sedimentation rate, which is slow for small ice crystals. This argument does not explain why the peak cloud fraction occurs below the cold point, however. Detrainment of ice that peaks below the tropopause is still necessary to get the cloud fraction to peak below the tropopause. The FAT hypothesis argues that this detrainment of ice is constrained by the radiative cooling efficiency.

Seeley et al. [60] present a critique of the fixed anvil temperature hypothesis in which they conclude that the evidence for it is weak, and that cloud temperature can vary in a model in which the basic physics of the FAT hypothesis are allowed to operate. Their argument is based on a set of simulations with a cloud-resolving model in which the cloud physics is simplified to include only condensation, evaporation, and a linear removal of condensed liquid water, and in which longwave cooling by water vapor is the only radiative process. Then, exploring a wide range of climates (surface temperatures from 260 to 310 K) in this simplified setting, the temperature at the level of maximum cloud cover or anvil temperature is found to increase as the surface temperature increases. They further argue that a “fixed” anvil temperature should be one that deviates no more than 1 K for a 10 K change in surface temperature. For surface temperatures above freezing, Seeley et al. find that the anvil temperature in their simplest model increases by about 4 K for every 10 K of surface temperature increase, a much larger change than in a model with more realistic physics. When more realistic cloud physics are used along with solar radiation and radiatively active CO₂ and clouds, the cloud fraction maximum remains much closer to a constant temperature, varying by 3 K for surface temperatures from 280 to 310 K. The differing response of anvil temperature in the simplified and more realistic settings argues that the vertical distribution of cloud is sensitive to some combination of sunlight, trace gases, ACRE, and the introduction of ice into the microphysics.

It is interesting that even for their simplified model, Seeley et al. [60] find that the upper level peak in detrainment estimated using the method of Romps and Kuang [61] remains within a couple of degrees of 220 K as the surface temperature is varied over the range of temperatures most relevant to the present climate (290 to 310 K), as is predicted by the FAT hypothesis. As the surface temperature is lowered below

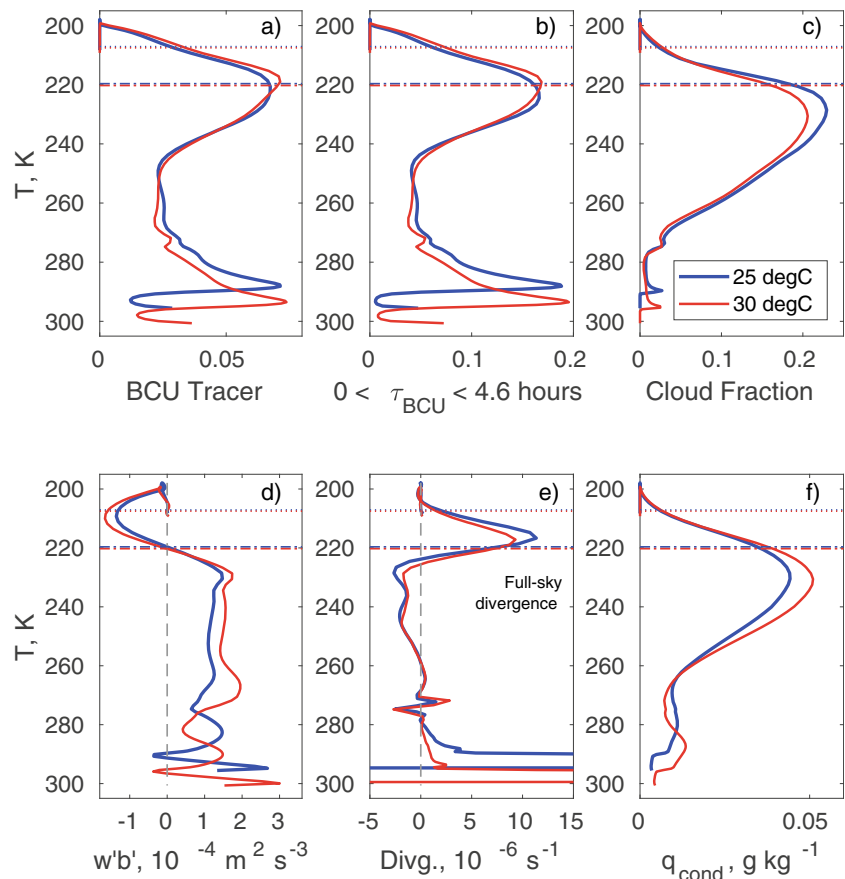
280 K, the detrainment peak occurs at significantly colder temperatures. A more dramatic transition occurs between surface temperatures of 270 K and 260 K, during which the upper-level cloud maximum occurs at a much colder temperature. At temperatures below freezing, the equilibrium Bowen ratio [62] gets large, so that energy fluctuations are dominated by temperature rather than humidity. The lapse rate approaches the dry adiabatic within the troposphere, and the fundamental character of the convection is changed toward that of dry convection [63], rather than the weak, nearly equilibrated convection of the warm tropical oceans that is highly modified by moist processes. In such cold cases, the lapse rate within the troposphere approaches the dry adiabatic lapse rate and subsidence is not constrained by the radiative cooling rate. This condition does not occur on Earth.

Here, we present some tracer experiments to show that freshly uplifted air containing ice is more efficiently delivered to the upper troposphere at an air temperature that is nearly independent of surface temperature. We offer this as a counterpoint to the Seeley et al. [60] argument that evaporation is more important than detrainment in defining the peak in cloud amount. We consider a tracer experiment in which cloudy updrafts are given a tracer value set to 1, which then decays with an e-folding time of 2 h once the air is no longer in the updraft. Figure 1 shows results obtained with the SAM model [64] with a 96 × 96-km domain with 144 vertical levels, RRTMG radiation [65] and P3 microphysics from Morrison and Milbrandt [66]. The simulation includes a tracer that is set to one inside buoyant, cloudy updrafts ($w > 1 \text{ m s}^{-1}$), and decays elsewhere with a timescale of 2 h. Figure 1a shows the mean value of the tracer, and Fig. 1b shows the area fraction for which the tracer value is between 0.1 and 0.999, or air that has been within a buoyant updraft less than 4.6 h ago. Both of these peaks near 220 K for both surface temperature specifications. Our assumption is that freshly detrained updraft air is more likely to contain ice and would correspond roughly to cloudy air.

The small area of recently buoyant air in the mid troposphere indicates that not much buoyant air is detrained there. One likely explanation is that the majority of the entrained air was previously detrained and so carries some of the characteristics of the plume air, rather than the undisturbed environment. Plumes of deep convection tend to be surrounded by a shell of air that has recently been modified by moist convection [67], similar to what is observed for shallow convection [68]. This can isolate the updraft from the full effect of the dry environment. The shell is produced by the efficient evaporation of detrained condensed water, which makes it more dense but also more humid than the environment.

Figure 1d shows the buoyancy flux in units of $\text{m}^2 \text{ s}^{-3}$, which is fairly constant up to the level where the temperature reaches 230 K, after which it passes through zero at about 220 K, peaks negative at about 210 K, and returns to zero at

Fig. 1 Buoyant cloudy updraft tracer experiment for RCE above SSTs of 25 °C and 30 °C. **a** Abundance of buoyant cloudy updraft tracer. **b** Fractional area covered by air that has recently been in a buoyant updraft. **c** Cloud fraction. **d** Buoyancy flux ($10^{-4} \text{ m}^2 \text{ s}^{-3}$). **e** Radiatively driven divergence (10^{-6} s^{-1}). **f** Mass of condensed water (g kg^{-1}). Dashed lines indicate the level at which the buoyancy flux first crosses zero in the upper troposphere (see panel **d**); dotted lines indicate the level of zero radiative cooling



200 K. The downward buoyancy flux at the top of the convective layer has been discussed by Kuang and Bretherton [69]. The temperature where the buoyancy flux crosses zero remains approximately constant, as does the temperature where the downward buoyancy flux goes to zero at the top of the overshoot layer. The maximum downward buoyancy flux must be close to the level where the radiative cooling rate crosses zero, since the divergence of the buoyancy flux is balancing the radiative heating rate. The temperatures of zero buoyancy flux and zero heating rate change by no more than a degree or two, while the air temperature at a fixed pressure in the upper troposphere changes by more than 10 K for a 5 K surface temperature change.

The temperature of buoyancy flux reversal marks the top of the well-mixed layer, which is defined as the layer in which radiation can efficiently remove the energy supplied by the buoyancy flux, which is constrained by the abundance of water vapor, which in turn is closely constrained by the temperature. This boundary is reasonably well marked by the radiatively driven divergence defined as in Kuang and Hartmann [15] (Fig. 1e), except here, we have used the full-sky radiation. The clear-sky radiative divergence is very similar, since the area occupied by optically thick cloud is relatively small, but ACRE is not negligible. It will be interesting to investigate whether ACRE weakens or strengthens the FAT

constraint. When the updraft loses buoyancy at the top of the efficiently cooled layer, detrainment of moist air is enhanced and the area covered by ice cloud is enhanced. A change in the stability occurs at the top of the well-mixed layer, as observed [55], and is marked by a change in buoyancy flux.

Figure 1c shows the cloud fraction defined as the part of the domain in which the condensed water mass is greater than $10^{-2} \text{ g kg}^{-1}$. The cloud fraction is sensitive to this limit on the water mass, since the overshoot layer contains a thin veil of ice cloud in these simulations. The overshooting convection that reaches the stable layer and produces the negative buoyancy flux there also carries with it some ice, of which the small particles are only slowly removed by sedimentation and evaporation [59]. The cloud fraction decreases rapidly upward with decreasing temperature in the overshoot layer, but more slowly downward with increasing temperature in the layer with upward buoyancy flux. The area occupied by recently buoyant air (Fig. 1b) shows a strong peak in the boundary layer and another peak at the top of the tropospheric mixed layer. The top of the tropospheric mixed layer remains at a nearly constant temperature as the SST is varied between 25 °C and 30 °C, as predicted by the FAT hypothesis, and the cloud fraction and ice mass peak just below that level. The temperature of the coldest cloud varies a little, but not more than 10–20% of the temperature of the air at a fixed pressure in the

upper troposphere. It is easy to imagine that details of the cloud microphysics could alter the vertical structure of the cloud fraction.

A critical factor in determining the dependence of cloud on temperature is the temperature depth of the overshoot layer, since small amounts of ice are injected into this layer by the overshooting convection, and if the particle size is small, the ice can stay there for a long time. The temperature depth of the overshoot layer in these simulations is relatively small, 20 K, but by modifying the conditions of the simulation, the temperature depth of the overshoot layer can be increased and thus provide ice to colder temperatures than in this simulation that includes all radiatively important gasses, realistic microphysics, and both solar and terrestrial radiative effects.

Global Models in RCE

Recently, RCE experiments have been conducted with global climate models, both with fixed SST and with an underlying slab ocean model. In these experiments, the rotation is set to zero and the insolation is set to a uniform tropical value, creating what might be called a “Tropic World” simulation [70–74]. Convection aggregates in these simulations such that separated large regions with active convection and others with no convection at all develop and interact. Such experiments can be conducted with a wide range of fixed SSTs or by forcing a model with a slab ocean with a wide range of CO₂ concentrations or solar irradiances. The purpose of such experiments can be to test how the convection parameterization behaves under such conditions or, more optimistically, to try to learn something about how the climate system works. Low cloud feedbacks in the subsiding regions are also quite important in these simulations.

Bony et al. [75] used fixed SST experiments to see how the convective cloud altitude and high cloud fraction responds to warmer temperatures. The cloud top temperature remained about the same, following the FAT hypothesis [14], but the high cloud fraction decreased at very high temperatures. The explanation offered was based on the increase of the dry static stability of the moist adiabatic temperature profile, which is ostensibly a different explanation than the explanation based on the reduced convective mass flux required to balance radiative cooling of the atmosphere [10]. A reduction in cloud area could constitute a negative feedback if it decreases the average humidity of the atmosphere and thereby tempers the water vapor feedback. The cloud feedback is completely uncertain because the net radiative effect of tropical convective clouds at the top of the atmosphere is small, and we do not know if or how this would change with warming. At present, we do not know exactly why the net radiative effect of tropical convective clouds is small, and consequently, we do not know whether this balance is likely to change in a warmed climate [17].

The small impact of convective clouds on the Earth’s radiative energy balance results from offsetting negative and positive contributions from thick, rainy anvil clouds and thinning cirrus clouds connected to them [19]. It is not yet known whether the small net cloud radiative effect of tropical convective clouds is a coincidence [76] and might change in a warmed climate or is the result of a feedback process [77] and might remain small in a changed climate [52, 78]. Simplified eddy-resolving modeling suggests that interactions among cloud radiative heating, turbulence, and cloud physics within extended upper-level ice clouds are critical in determining their properties, and that these processes are probably not well simulated in global climate models [18]. Global climate models in Tropic World mode can, however, investigate the mechanisms connecting, SST, cloud radiative effects, and atmospheric circulations as hypothesized by Hartmann et al. [77].

Global climate models run in Tropic World mode above slab oceans reveal interesting interactions that may provide valuable lessons about how convection, clouds, circulation, and the energy balance interact to determine tropical climate [70–73]. In such experiments, the convection aggregates and interacts with the SST in a way that is fairly consistent across different models, so that some behaviors seem to be independent of parameterization details. Sensitivity to the convective parameterization has been demonstrated in at least one model [79]. The degree of self-aggregation and associated SST contrast in the models varies with time between a highly aggregated state with a large SST contrast and a less aggregated state with a smaller SST contrast [72]. The time and space scales of the oscillation depend on the heat capacity of the slab ocean model and the strengths of the feedbacks within the model.

Tropic World simulations with interactive SST suggest that as the Earth warms, convection is confined to a smaller fraction of the global area. Since this means a larger fraction of the globe experiences subsidence and the associated dry upper troposphere, it may seem that the sensitivity of aggregation to mean temperature would provide a negative feedback. In climate models, however, other interactions can intervene, especially in the case in which the SST is allowed to respond to the resulting energetic and circulation changes. As an example, Coppin and Bony [80] note that as aggregation occurs and SST gradients develop, low clouds can respond to both the mean SST and the SST gradients within the domain.

Oscillations that occur in global Tropic world simulations with slab oceans may provide insight into how SST variability, large-scale circulations, clouds, and evaporation interact to maintain the tropical climate that includes a large region of almost uniform warm temperature, within which the top-of-atmosphere cloud radiative effects are small and uniform. For example, Fig. 2 shows composites of the anomalies of temperature and energy fluxes for two simulations (Table 1) with the GFDL AM2 model with a slab ocean with the heat

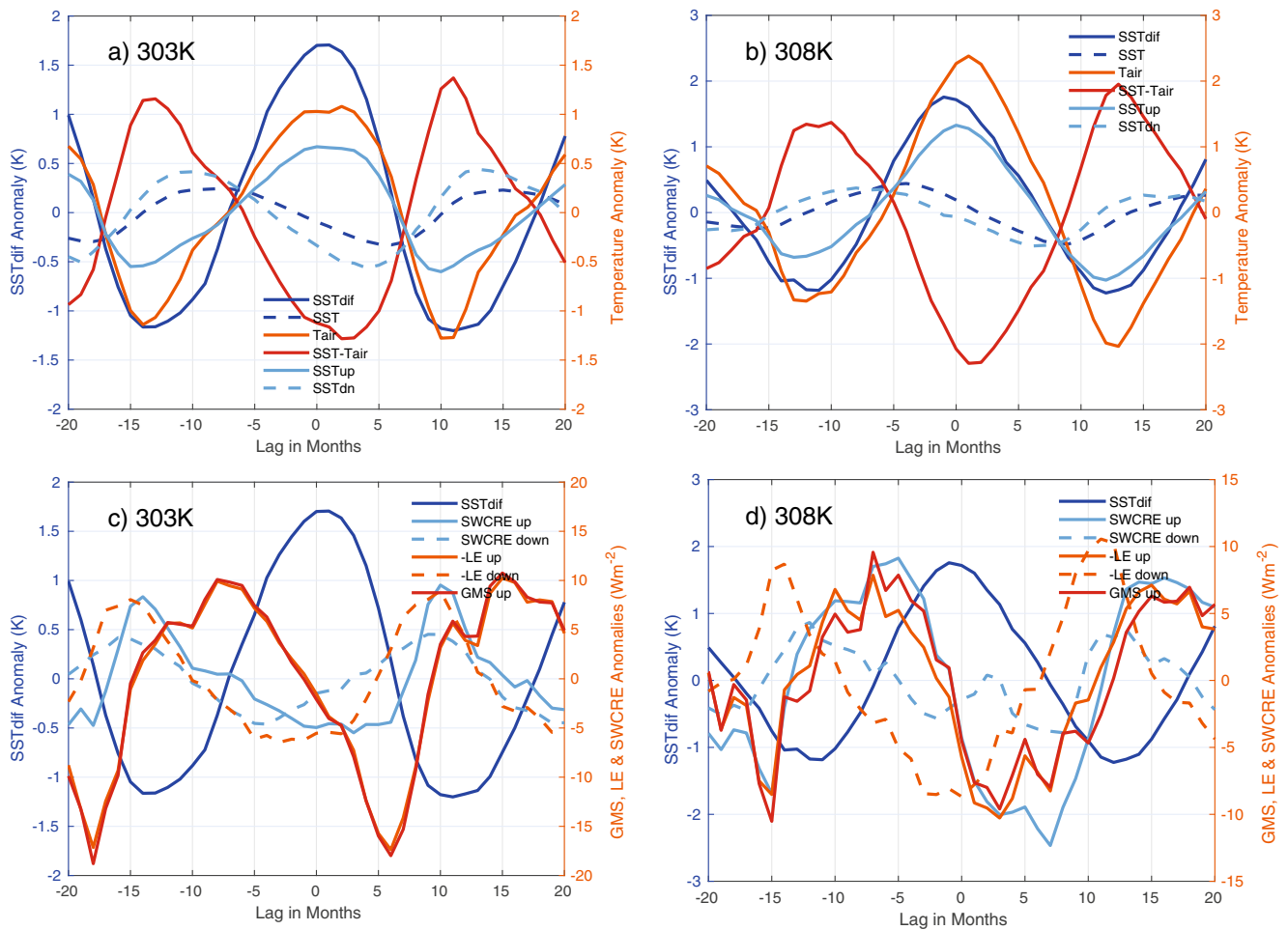


Fig. 2 Temperature anomalies (a, b) and energy flux anomalies (c, d) composited according to the difference between the warmest and coldest quintiles of SST (SSTdif) for simulations with mean SST of 302.8 K (303 K: a, c) and 307.9 K (308 K: b, d). SST and Tair are the global average SST and global average mass-averaged air temperature. SST up is the SST averaged over the region where the mass-averaged vertical velocity is upward and the converse for SST down. SWCRE is the

shortwave cloud radiative effect. The horizontal energy transport from the convective regions is measured here by the gross moist stability, the net atmospheric energy divergence from regions of upward motion. LE is the rate at which latent energy is transferred from the surface to the atmosphere and is plotted with negative sign so that its relationship to the Gross Moist Stability in the region of upward motion (GMSup) can be more easily seen

capacity of 50 m of water. In this configuration, the model produces a coherent 22-month periodicity in which the SST contrast between the warmest and coldest quintiles of SST varies by almost 3 K and the subsiding fraction also varies by about 8%, much as described by Coppin and Bony [72] for the LMDZ5A-LR GCM. In this case, we have used SST difference across the model domain as the compositing variable, referencing all other changes to maxima in the SST difference.

The subsiding fraction variation is almost in phase with the SST difference (not shown).

The air temperature also undergoes a cycle, with the warmest air temperature at the time of the maximum SST difference, which is when the global precipitation rate is maximized. Since the global mean SST varies much less than the contrast in SST or the air temperature, the difference between the global mean SST and the global mean air

Table 1 Mean parameters for 303 K and 308 K cases. SSTdif is the mean difference between the warmest and coldest quintiles of SST, SF is subsiding fraction, RH is mass-averaged percent relative humidity. The SST change between the two cases is forced by insolation changes

Case	Insolation Wm ⁻²	SST K	SSTdif K	Precip mm day ⁻¹	SF	RH percent	OLR Wm ⁻²	Albedo
303 K	349.3	302.8	4.65	4.45	0.67	44.6	273.6	0.22
308 K	364.4	307.9	5.23	5.40	0.70	43.7	289.9	0.21

temperature also has large variations, which affect the efficiency of energy transport in the atmosphere. A cooler and warmer case is simulated by changing the insolation (Table 1). During the limit cycle, the SST under the upward motion gradually increases until the SST contrast reaches a maximum, then declines. In the cooler case (303 K), the reason for the decline is primarily the rapid increase of evaporative cooling rate in the upward region, which in turn is supported by the enhanced export of energy in the atmosphere. In the warmer case (308 K), the phasing is different, and the shortwave cloud radiative effect in the region of upward motion becomes as important as the evaporative cooling in suppressing the warmest SST at the end of the warming cycle. In each case, after the warm pool has been broken and the SST contrast is at a minimum, evaporation and reflection of radiation by clouds decrease in both the upward and downward regions, the global mean SST begins to increase, and subsequently, the SST contrasts begin to rebuild.

The cycle of greater aggregation, greater SST difference, and associated more rapid hydrological cycling results from instabilities similar to those that lead to aggregation of convection in fixed SST models, but it is brought to an end in these experiments by some combination of energy export from the warm region and the reduction of surface insolation by cloud reflection within the warm region. Both of these effects probably arise from basic thermodynamic constraints, but both are also sensitive to the parameterizations within the climate model. In the 308 K case, cloud shading of surface shortwave radiation is as important as evaporation in suppressing the warm pool at the end of the warming cycle. The increased importance of shortwave cloud forcing in the 308 K experiment compared to the 303 K experiment is at least in part related to an increase of grid-scale storms in the warmer case. As the surface warms, the rainfall in the AM2 model comes increasingly from the large-scale scheme compared to the convective parameterization [26]. A substantial increase in the fraction of the precipitation that comes from the large-scale parameterization occurs between the 303 K and 308 K cases, which means that grid cells become saturated and the cloud albedo increases. The relative importance of cloud radiative effects versus atmospheric transport in constraining the maximum SST in the Tropics is worthy of further study.

Tropic World simulations are fun and interesting, but it is as yet unclear whether they can lead to fundamental understanding of how the climate system works, or even whether they can help improve the quality of parameterizations. The model setup is very different from the observed situation of a rotating planet with the warm pool on the equator. Nonetheless, the model setup does provide an interesting laboratory for exploring interactions of convection, clouds, large-scale circulation, and SST.

Conclusion

At the mean temperature of the Earth's surface, the change in latent energy of a saturated parcel of air is about twice the internal energy change associated with the temperature change, and in the Tropics, the proportion is four to one. Water vapor is also the primary greenhouse gas. Moisture thus plays a central role in the energetics of the climate system and its change. Much of what we robustly understand about the mechanisms of climate change is based on the dependence of saturation vapor density on temperature, and on the phase changes of water. An example is the quality of the assumption of fixed relative humidity, which leads robustly to a strong positive water vapor greenhouse effect feedback. Other examples likely include rising convective cloud tops and a deepening of the troposphere in a warmed climate. The dependence of saturation vapor pressure on temperature causes the well-mixed layer of the troposphere to have an almost constant top temperature.

Much of what is uncertain in climate science also results from the role of water in the climate system. Despite knowing the dependence on temperature at equilibrium of saturation vapor pressure and the phase of water, we are uncertain why the atmosphere contains the exact amounts of liquid water and ice that it does and how this condensed water is distributed in space. Condensed water has strong impacts on the absorption and emission of radiation by Earth. If we cannot predict with certainty how the condensed water in the atmosphere will change with the climate, then our assessment of climate sensitivity will remain uncertain. Reducing this uncertainty requires understanding how radiation, cloud physics, and atmospheric motion interact to determine the suspended condensate. Work with process models that can better resolve these interactions can lead to understanding and conceptual theories that can be used to constrain the possible responses. Progress is being made, but much remains to be done.

Acknowledgments The authors thank Tim Cronin and an anonymous reviewer for very helpful comments and suggestions.

Funding Support was from the National Science Foundation under Grant AGS-1549579 and from the Regional and Global Climate Modeling Program of the Office of Science of the U.S. Department of Energy (DE-SC0012580).

Compliance with Ethical Standards

Conflict of Interest The authors state that there are no conflicts of interest.

References

1. Manabe S, Wetherald RT. Thermal equilibrium of the atmosphere with a given distribution of relative humidity. *J Atmos Sci.* 1967;24: 241–59.

2. Raval A, Ramanathan V. Observational determination of the greenhouse effect. *Nature*. 1989;342(6251):758–61.
3. Soden BJ, Wetherald RT, Stenchikov GL, Robock A. Global cooling after the eruption of Mount Pinatubo: a test of climate feedback by water vapor. *Science*. 2002;296(APR 26 2002):727–30.
4. Koll DDB, Cronin TW. Earth's outgoing longwave radiation linear due to H_2O greenhouse effect. *Proc Natl Acad Sci U S A*. 2018;115:10293–8. <https://doi.org/10.1073/pnas.1809868115>.
5. Romps DM. An analytical model for tropical relative humidity. *J Clim*. 2014;27(19):7432–49. <https://doi.org/10.1175/jcli-d-14-00255.1>.
6. Pierrehumbert RT. Thermostats, radiator fins and the local runaway greenhouse. *J Atmos Sci*. 1995;52:1784–806.
7. Sherwood SC. Maintenance of the free-tropospheric tropical water vapor distribution. 2. Simulation by large-scale advection. *J Clim*. 1996;9(V 1996):2919–34.
8. Salathé EP, Hartmann DL. A trajectory analysis of tropical upper-tropospheric moisture and convection. *J Clim*. 1997;10(OCT 1997):2533–47.
9. Ming Y, Held IM. Modeling water vapor and clouds as passive tracers in an idealized GCM. *J Clim*. 2018;31(2):775–86. <https://doi.org/10.1175/jcli-d-16-0812.1>.
10. Held IM, Soden BJ. Robust responses of the hydrological cycle to global warming. *J Clim*. 2006;19(21):5686–99.
11. Pendergrass AG, Hartmann DL. The atmospheric energy constraint on global-mean precipitation change. *J Clim*. 2014;27(2):757–68. <https://doi.org/10.1175/jcli-d-13-00163.1>.
12. Jeevanjee N, Romps DM. Mean precipitation change from a deepening troposphere. *Proc Natl Acad Sci U S A*. 2018;115(45):11465–70. <https://doi.org/10.1073/pnas.1720683115>.
13. Bretherton CS, Blossey PN, Khairoutdinov M. An energy-balance analysis of deep convective self-aggregation above uniform SST. *J Atmos Sci*. 2005;62(12):4273–92.
14. Hartmann DL, Larson K. An important constraint on tropical cloud-climate feedback. *Geophys Res Lett*. 2002;29(20):1951–4. <https://doi.org/10.1029/2002GL015835>.
15. Kuang Z, Hartmann DL. Testing the fixed anvil temperature hypothesis in a cloud-resolving model. *J Clim*. 2007;20:2051–7. <https://doi.org/10.1175/JCLI14124.1>.
16. Zelinka MD, Hartmann DL. Why is longwave cloud feedback positive? *J Geophys Res Atmos*. 2010;115:D16117. <https://doi.org/10.1029/2010jd013817>.
17. Hartmann DL. Tropical anvil clouds and climate sensitivity. *Proc Natl Acad Sci U S A*. 2016;113(32):8897–9. <https://doi.org/10.1073/pnas.1610455113>.
18. Hartmann DL, Gasparini B, Berry SE, Blossey PN. The life cycle and net radiative effect of tropical anvil clouds. *J Adv Model Earth Sys*. 2018;0(0). doi:doi:<https://doi.org/10.1029/2018MS001484>.
19. Hartmann DL, Berry SE. The balanced radiative effect of tropical anvil clouds. *J Geophys Res Atmos*. 2017;122(9):5003–20. <https://doi.org/10.1002/2017jd026460>.
20. Held IM, Hemler RS, Ramaswamy V. Radiative-convective equilibrium with explicit two-dimensional moist convection. *J Atmos Sci*. 1993;50(23):3909–27.
21. Tompkins AM, Craig GC. Radiative-convective equilibrium in a three-dimensional cloud-ensemble model. *Quart J Roy Meteorol Soc*. 1998;124(550):2073–97.
22. Tompkins AM, Craig GC. Time-scales of adjustment to radiative-convective equilibrium in the tropical atmosphere. *Quart J Royal Meteorol Soc*. 1998;124(552):2693–713.
23. Tompkins AM, Craig GC. Sensitivity of tropical convection to sea surface temperature in the absence of large-scale flow. *J Clim*. 1999;12(2):462–76.
24. Tompkins AM. On the relationship between tropical convection and sea surface temperature. *J Clim*. 2001;14(5):633–7. [https://doi.org/10.1175/1520-0442\(2001\)014<0633:otrbc>2.0.co;2](https://doi.org/10.1175/1520-0442(2001)014<0633:otrbc>2.0.co;2).
25. Su H, Bretherton CS, Chen SS. Self-aggregation and large-scale control of tropical deep convection: a modeling study. *J Atmos Sci*. 2000;57(JUN 1 2000):1797–816.
26. Held IM, Zhao M, Wyman B. Dynamic radiative-convective equilibria using GCM column physics. *J Atmos Sci*. 2007;64(1):228–38.
27. Tompkins AM. Organization of tropical convection in low vertical wind shears: the role of water vapor. *J Atmos Sci*. 2001;58(6):529–45. [https://doi.org/10.1175/1520-0469\(2001\)058<0529:ootcil>2.0.co;2](https://doi.org/10.1175/1520-0469(2001)058<0529:ootcil>2.0.co;2).
28. Wing AA, Emanuel KA. Physical mechanisms controlling self-aggregation of convection in idealized numerical modeling simulations. *J Adv Model Earth Sys*. 2014;6(1):59–74. <https://doi.org/10.1002/2013ms000269>.
29. Muller CJ, Held IM. Detailed investigation of the self-aggregation of convection in cloud-resolving simulations. *J Atmos Sci*. 2012;69(8):2551–65. <https://doi.org/10.1175/jas-d-11-0257.1>.
30. Craig GC, Mack JM. A coarsening model for self-organization of tropical convection. *J Geophys Res Atmos*. 2013;118(16):8761–9. <https://doi.org/10.1002/jgrd.50674>.
31. Muller C, Bony S. What favors convective aggregation and why? *Geophys Res Lett*. 2015;42(13):5626–34. <https://doi.org/10.1002/2015gl064260>.
32. Jeevanjee N, Romps DM. Convective self-aggregation, cold pools, and domain size. *Geophys Res Lett*. 2013;40(5):994–8. <https://doi.org/10.1002/grl.50204>.
33. Cronin TW, Wing AA. Clouds, circulation, and climate sensitivity in a radiative-convective equilibrium channel model. *J Adv Model Earth Sys*. 2017;9(8):2883–905. <https://doi.org/10.1002/2017ms001111>.
34. Neelin JD, Sahany S, Stechmann SN, Bernstein DN. Global warming precipitation accumulation increases above the current-climate cutoff scale. *Proc Natl Acad Sci U S A*. 2017;114(6):1258–63. <https://doi.org/10.1073/pnas.1615333114>.
35. Muller CJ, O'Gorman PA, Back LE. Intensification of precipitation extremes with warming in a cloud-resolving model. *J Clim*. 2011;24(11):2784–800. <https://doi.org/10.1175/2011jcli3876.1>.
36. Romps DM. Response of tropical precipitation to global warming. *J Atmos Sci*. 2011;68(1):123–38. <https://doi.org/10.1175/2010jas3542.1>.
37. Singh MS, O'Gorman PA. Influence of microphysics on the scaling of precipitation extremes with temperature. *Geophys Res Lett*. 2014;41(16):6037–44. <https://doi.org/10.1002/2014gl061222>.
38. Pfahl S, O'Gorman PA, Fischer EM. Understanding the regional pattern of projected future changes in extreme precipitation. *Nature Climate Change*. 2017;7(6):423–+. <https://doi.org/10.1038/nclimate3287>.
39. Nie J, Sobel AH, Shaevitz DA, Wang SG. Dynamic amplification of extreme precipitation sensitivity. *Proc Natl Acad Sci U S A*. 2018;115(38):9467–72. <https://doi.org/10.1073/pnas.1800357115>.
40. Singh MS, O'Gorman PA. Increases in moist-convective updraft velocities with warming in radiative-convective equilibrium. *Quart J Roy Meteorol Soc*. 2015;141(692):2828–38. <https://doi.org/10.1002/qj.2567>.
41. Singh MS, O'Gorman PA. Influence of entrainment on the thermal stratification in simulations of radiative-convective equilibrium. *Geophys Res Lett*. 2013;40(16):4398–403. <https://doi.org/10.1002/grl.50796>.
42. Singh MS, Kuang ZM, Maloney ED, Hannah WM, Wolding BO. Increasing potential for intense tropical and subtropical thunderstorms under global warming. *Proc Natl Acad Sci U S A*. 2017;114(44):11657–62. <https://doi.org/10.1073/pnas.1707603114>.
43. Seeley JT, Romps DM. Why does tropical convective available potential energy (CAPE) increase with warming? *Geophys Res Lett*. 2015;42(23). <https://doi.org/10.1002/2015gl066199>.
44. Bretherton CS, Park S. A new bulk shallow-cumulus model and implications for penetrative entrainment feedback on updraft

- buoyancy. *J Atmos Sci.* 2008;65(7):2174–93. <https://doi.org/10.1175/2007jas2242.1>.
45. Bretherton CS. Insights into low-latitude cloud feedbacks from high-resolution models. *Phil Trans Roy Soc A.* 2015;373(2054). <https://doi.org/10.1098/rsta.2014.0415>.
 46. Stevens B, Bony S, Webb M. Clouds on-off climate intercomparison experiment (COOKIE). Tech. rep.2013.
 47. Harrop BE, Hartmann DL. The role of cloud radiative heating in determining the location of the ITCZ in Aquaplanet simulations. *J Clim.* 2016;29(8):2741–63. <https://doi.org/10.1175/jcli-d-15-0521.1>.
 48. Watt-Meyer O, Frierson DMW. Local and remote impacts of atmospheric cloud radiative effects onto the eddy-driven jet. *Geophys Res Lett.* 2017;44(19):10,036–10,44. <https://doi.org/10.1002/2017GL074901>.
 49. Voigt A, Shaw TA. Impact of regional atmospheric cloud radiative changes on shifts of the extratropical jet stream in response to global warming. *J Clim.* 2016;29(23):8399–421. <https://doi.org/10.1175/jcli-d-16-0140.1>.
 50. Ceppi P, Hartmann DL. Clouds and the atmospheric circulation response to warming. *JClimate.* 2016;29(2):783–99. <https://doi.org/10.1175/jcli-d-15-0394.1>.
 51. Dobbie S, Jonas P. Radiative influences on the structure and lifetime of cirrus clouds. *Quart J Roy Meteorol Soc.* 2001;127(578):2663–82. <https://doi.org/10.1256/smsqj.57807>.
 52. Wall CJ, Hartmann DL. Balanced cloud radiative effects across a range of dynamical conditions over the tropical West Pacific. *Geophys Res Lett.* 2018;45(20):11490–8. <https://doi.org/10.1029/2018gl080046>.
 53. Folkins I, Loewenstein M, Podolske J, Oltmans SJ, Proffitt M. A barrier to vertical mixing at 14 km in the tropics: evidence from ozonesondes and aircraft measurements. *J Geophys Res Atmos.* 1999;104(SEP 27 1999):22095–102.
 54. Hartmann DL, Holton JR, Fu Q. The heat balance of the tropical tropopause, cirrus, and stratospheric dehydration. *Geophys Res Lett.* 2001;28(10):1969–72.
 55. Folkins I. Origin of lapse rate changes in the upper tropical troposphere. *J Atmos Sci.* 2002;59(5):992–1005.
 56. Harrop BE, Hartmann DL. Testing the role of radiation in determining tropical cloud-top temperature. *JClimate.* 2012;25(17):5731–47. <https://doi.org/10.1175/jcli-d-11-00445.1>.
 57. Thompson DWJ, Bony S, Li Y. Thermodynamic constraint on the depth of the global tropospheric circulation. *Proc Nat Acad Sci U S A.* 2017;114(31):8181–6. <https://doi.org/10.1073/pnas.1620493114>.
 58. Thompson DWJ, Ceppi P, Yi Y. Testing a key constraint on extratropical tropopause height *J Climate.* 2018:submitted.
 59. Seeley JT, Jeevanjee N, Langhans W, Romps DM. Formation of tropical anvil clouds by slow evaporation. *Geophys Res Lett* 0(0). <https://doi.org/10.1029/2018GL080747>.
 60. Seeley JT, Jeevanjee N, Romps DM. FAT or FiTT: are anvil clouds or the tropopause temperature-invariant? *Geophys Res Lett.*0(ja). <https://doi.org/10.1029/2018GL080096>.
 61. Romps DM, Kuang ZM. Do undiluted convective plumes exist in the upper tropical troposphere? *J Atmos Sci.* 2010;67(2):468–84. <https://doi.org/10.1175/2009jas3184.1>.
 62. Hartmann DL. *Global Physical Climatology.* 2nd ed. Elsevier; 2016.
 63. de Rooy WC, Bechtold P, Frohlich K, Hohenegger C, Jonker H, Mironov D, et al. Entrainment and detrainment in cumulus convection: an overview. *Q J R Meteorol Soc.* 2013;139(670):1–19. <https://doi.org/10.1002/qj.1959>.
 64. Khairoutdinov MF, Randall DA. Cloud resolving modeling of the ARM summer 1997 IOP: model formulation, results, uncertainties, and sensitivities. *J Atmos Sci.* 2003;60(4):607–25.
 65. Clough SA, Shephard MW, Mlawer E, Delamere JS, Iacono M, Cady-Pereira K, et al. Atmospheric radiative transfer modeling: a summary of the AER codes. *J Quant Spectros Rad Trans.* 2005;91(2):233–44. <https://doi.org/10.1016/j.jqsrt.2004.05.058>.
 66. Morrison H, Milbrandt JA. Parameterization of cloud microphysics based on the prediction of bulk ice particle properties. Part I: scheme description and idealized tests. *J Atmos Sci.* 2015;72(1):287–311. <https://doi.org/10.1175/jas-d-14-0065.1>.
 67. Glenn IB, Krueger SK. Downdrafts in the near cloud environment of deep convective updrafts. *J Adv Model Earth Sys.* 2014;6(1):1–8. <https://doi.org/10.1002/2013ms000261>.
 68. Katzwinkel J, Siebert H, Heus T, Shaw RA. Measurements of turbulent mixing and subsiding shells in trade wind cumuli. *J Atmos Sci.* 2014;71(8):2810–22. <https://doi.org/10.1175/jas-d-13-0222.1>.
 69. Kuang ZM, Bretherton CS. Convective influence on the heat balance of the tropical tropopause layer: a cloud-resolving model study. *J Atmos Sci.* 2004;61(23):2919–27.
 70. Popke D, Stevens B, Voigt A. Climate and climate change in a radiative-convective equilibrium version of ECHAM6. *J Adv Model Earth Sys.* 2013;5(1):1–14. <https://doi.org/10.1029/2012ms000191>.
 71. Reed KA, Medeiros B, Bacmeister JT, Lauritzen PH. Global radiative-convective equilibrium in the community atmosphere model, version 5. *J Atmos Sci.* 2015;72(5):2183–97. <https://doi.org/10.1175/jas-d-14-0268.1>.
 72. Coppin D, Bony S. Internal variability in a coupled general circulation model in radiative-convective equilibrium. *Geophys Res Lett.* 2017;44(10):5142–9. <https://doi.org/10.1002/2017gl073658>.
 73. Hohenegger C, Stevens B. Coupled radiative convective equilibrium simulations with explicit and parameterized convection. *J Adv Model Earth Sys.* 2016;8(3):1468–82. <https://doi.org/10.1002/2016ms000666>.
 74. Arnold NP, Putman WM. Nonrotating convective self-aggregation in a limited area AGCM. *J Adv Model Earth Sys.* 2018;10(4):1029–46. <https://doi.org/10.1002/2017ms001218>.
 75. Bony S, Stevens B, Coppin D, Becker T, Reed K, Voigt A, et al. Thermodynamic control of anvil-cloud amount. *Proc Nat Acad Sci U S A.* 2016;113(32):8927–32. <https://doi.org/10.1073/pnas.1601472113>.
 76. Kiehl JT. On the observed near cancellation between longwave and shortwave cloud forcing in tropical regions. *J Clim.* 1994;7(4):559–65.
 77. Hartmann DL, Moy LA, Fu Q. Tropical convection and the energy balance at the top of the atmosphere. *J Clim.* 2001;14(24):4495–511. [https://doi.org/10.1175/1520-0442\(2001\)014<4495:TCATEB>2.0.CO;2](https://doi.org/10.1175/1520-0442(2001)014<4495:TCATEB>2.0.CO;2).
 78. Wall CJ, Hartmann DL, Thieman MM, Smith WL, Minnis P. The life cycle of anvil clouds and the top-of-atmosphere radiation balance over the tropical West Pacific. *J Clim.* 2018;31(24):10059–80. <https://doi.org/10.1175/jcli-d-18-0154.1>.
 79. Becker T, Stevens B, Hohenegger C. Imprint of the convective parameterization and sea-surface temperature on large-scale convective self-aggregation. *J Adv Model Earth Sys.* 2017;9(2):1488–505. <https://doi.org/10.1002/2016ms000865>.
 80. Coppin D, Bony S. On the interplay between convective aggregation, surface temperature gradients, and climate sensitivity. *J Adv Model Earth Sys.* 2018;10(12):3123–38. <https://doi.org/10.1029/2018MS001406>.